

# Influence of tetramethylammonium hydroxide on niobium nitride thin films

Emily Toomey, Marco Colangelo, Navid Abedzadeh, and Karl K. Berggren

Citation: *Journal of Vacuum Science & Technology B* **36**, 06JC01 (2018); doi: 10.1116/1.5047427

View online: <https://doi.org/10.1116/1.5047427>

View Table of Contents: <http://avs.scitation.org/toc/jvb/36/6>

Published by the [American Vacuum Society](#)

---

---

**HIDEN**  
ANALYTICAL

## Instruments for Advanced Science

Contact Hiden Analytical for further details:

**W** [www.HidenAnalytical.com](http://www.HidenAnalytical.com)

**E** [info@hiden.co.uk](mailto:info@hiden.co.uk)

**CLICK TO VIEW** our product catalogue



### Gas Analysis

- ▶ dynamic measurement of reaction gas streams
- ▶ catalysis and thermal analysis
- ▶ molecular beam studies
- ▶ dissolved species probes
- ▶ fermentation, environmental and ecological studies



### Surface Science

- ▶ UHV TPD
- ▶ SIMS
- ▶ end point detection in ion beam etch
- ▶ elemental imaging - surface mapping



### Plasma Diagnostics

- ▶ plasma source characterization
- ▶ etch and deposition process reaction kinetic studies
- ▶ analysis of neutral and radical species



### Vacuum Analysis

- ▶ partial pressure measurement and control of process gases
- ▶ reactive sputter process control
- ▶ vacuum diagnostics
- ▶ vacuum coating process monitoring

# Influence of tetramethylammonium hydroxide on niobium nitride thin films

Emily Toomey,<sup>a)</sup> Marco Colangelo,<sup>a)</sup> Navid Abedzadeh, and Karl K. Berggren<sup>b)</sup>  
*Department of Electrical Engineering and Computer Science, Massachusetts Institute of Technology,  
Cambridge, Massachusetts 02139*

(Received 6 July 2018; accepted 1 October 2018; published 15 October 2018)

Functionality of superconducting thin-film devices such as superconducting nanowire single photon detectors stems from the geometric effects that take place at the nanoscale. The engineering of these technologies requires high-resolution patterning, often achieved with electron beam lithography. Common lithography processes using hydrogen silsesquioxane (HSQ) as the electron beam resist rely on tetramethylammonium hydroxide (TMAH) as both a developer and a resist adhesion promoter. Despite the strong role played by TMAH in the fabrication of superconducting devices, its potential influence on the superconducting films themselves has not yet been reported. In this work, the authors demonstrate that a 25% TMAH developer damages niobium nitride (NbN) thin films by modifying the surface chemistry and creating an etch contaminant that slows reactive ion etching in  $\text{CF}_4$ . They also show how the identity of the contaminant may be revealed through characterization including measurement of the superconducting film properties and Fourier transform infrared spectroscopy. Although workarounds may be available, the results reveal that processes using 25% TMAH as an adhesion promoter are not preferred for NbN films and that changes to the typical HSQ fabrication procedure will need to be made in order to prevent damage of NbN nanoscale devices. *Published by the AVS.* <https://doi.org/10.1116/1.5047427>

## I. INTRODUCTION

The ability to pattern superconducting films at the nanoscale via electron beam lithography (EBL) has enabled numerous technologies that take advantage of unique phenomena occurring at these critical dimensions. For instance, superconducting nanowire single photon detectors (SNSPDs) rely on the formation of a resistive hotspot across a nanowire width of  $\sim 100$  nm to signal a detection event.<sup>1</sup> More recently, the patterning of dimensions  $< 10$  nm has facilitated the development of a device that harnesses the current-crowding effect<sup>2</sup> in superconductors to nondestructively read out a memory state.<sup>3</sup> These lithographic advancements have thus pushed the applications of thin-film superconducting devices into the fields of detection, digital circuitry, and sensing.

Precise control of superconducting materials at nanoscale dimensions demands both a high-resolution EBL process and a superior electron beam resist. Hydrogen silsesquioxane (HSQ) is a negative tone electron beam resist often selected for these purposes due to its  $\sim 5$  nm resolution and minimal line edge roughness.<sup>4,5</sup> After patterning the HSQ, development is commonly done using solutions of the strong base tetramethylammonium hydroxide (TMAH); for instance, past processes have developed HSQ by submerging it in 25% TMAH for durations ranging from 1 to 4 min.<sup>6–9</sup> TMAH has also been used to pretreat films before spinning resist in order to activate the film surface and promote HSQ adhesion.<sup>10,11</sup>

Despite the prevalence of TMAH in the fabrication process for superconducting devices, its potential negative effects on the superconducting film itself have not been fully investigated. As a result, it is unknown whether TMAH damages films in a way that somehow limits superconducting device

performance. Prior literature showed that pretreating niobium nitride (NbN) films with 25% TMAH for 4 min increased the sheet resistance  $R_s$  and decreased the critical temperature  $T_c$ , suggesting degradation and potential thinning of the superconducting material.<sup>10</sup> However, no further studies have been made to verify or explain this observation. We were recently motivated to understand this phenomenon when we noticed that a thick NbN film (thickness  $d \sim 20$  nm) patterned with HSQ took nearly twice as long to etch in  $\text{CF}_4$  as an unpatterned control film, causing the HSQ mask to be almost entirely removed before the etch was complete (see Fig. 1). As this left the underlying NbN vulnerable to damage by reactive ion etching (RIE), it became clear that improved knowledge of the lithography process was needed to guarantee successful pattern transfer and device fidelity, especially for thick films.

In this work, we investigate the HSQ development process with NbN films and demonstrate that the observed discrepancy in etch time is caused by TMAH reacting with NbN, modifying the film's surface chemistry and reducing the thickness of the pure superconductor. As shown in Fig. 2, TMAH has an observable impact on the film's appearance, increasing the surface roughness and creating clusters of material that form a barrier to reactive ion etching in  $\text{CF}_4$ . The steps taken to uncover this new understanding are presented here as two primary experiments. In Experiment 1, we explore how exposure to TMAH hinders the reactive ion etching of NbN films and demonstrate how the effect may be ameliorated. In Experiment 2, we perform material analysis on both the superconducting film and the clusters forming at the surface to identify the etch contaminant species. Through these means, we show how the reaction that forms the surface contaminant deteriorates the critical parameters of the pure superconductor by consuming the film.

<sup>a)</sup>E. Toomey and M. Colangelo contributed equally to this work.

<sup>b)</sup>Author to whom correspondence should be addressed: [berggren@mit.edu](mailto:berggren@mit.edu)

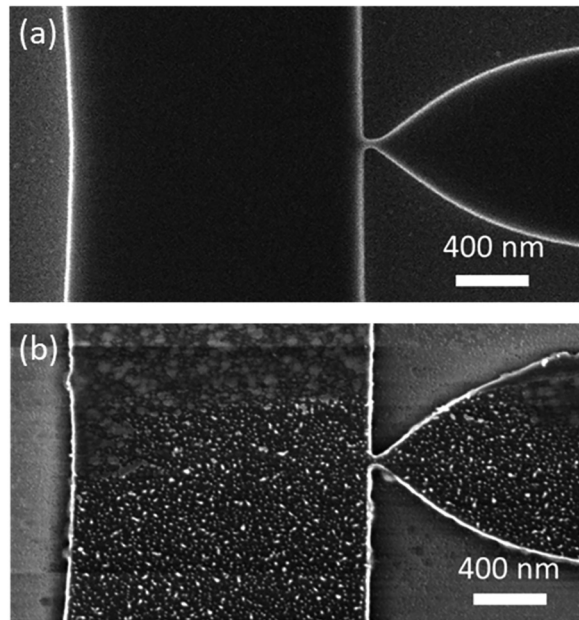


FIG. 1. Removal of HSQ mask due to prolonged reactive ion etching. (a) Scanning electron micrograph of a three-terminal superconducting device patterned with HSQ prior to RIE. (b) Scanning electron micrograph of the same device after the etching was complete (8 min). The rough surface suggests that the HSQ mask has been mostly removed, exposing the NbN film of the device and leaving it vulnerable to damage.

## II. EXPERIMENT 1: IMPACT ON ETCH RATE

### A. Methods

To investigate the impact of TMAH on the reactive ion etching of NbN, we exposed NbN samples diced from the same wafer to the 25% TMAH developer for various durations and measured their sheet resistances after etching as an indicator of remaining film thickness. An NbN film was first bias sputtered at room temperature on a 4 in. Si wafer in an AJA sputtering system following the procedure described in Ref. 12. The film had a sheet resistance of approximately  $90 \Omega/\text{square}$ , a critical temperature of 8.1 K, and a thickness of  $\sim 20$  nm. After dicing the wafer into 1 cm square samples, the samples were cleaned in acetone, methanol, and isopropyl alcohol (IPA). Once cleaned, we submerged each sample in 25% TMAH for durations ranging from 0 to 90 s. To stop

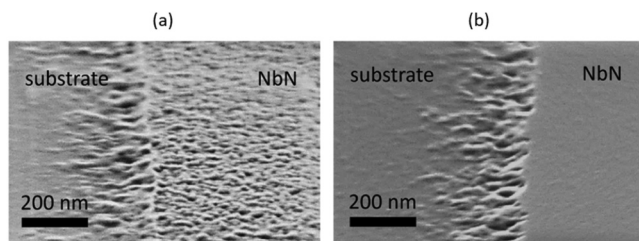


FIG. 2. Modification of the NbN surface by TMAH. Scanning electron micrographs reveal the difference in surface features between an NbN film that has been submerged in 25% TMAH for 4 h (a) and one that has been untreated (b). The ridge in both images represents the edge of a pattern made via photolithography to serve as a reference point for imaging. The treated sample was immersion rinsed in deionized water for 30 s following exposure to TMAH.

exposure to TMAH, the samples were rinsed in deionized (DI) water for either the traditional 30 s used in our standard process or for 3 min under a constantly running DI stream. Samples were then briefly rinsed in IPA, another step used in our conventional HSQ process to reduce surface tension. No HSQ was applied at any step of the process.

Following exposure to TMAH, the samples were reactively ion etched in a Plasmatherm RIE in  $\text{CF}_4$  for 2.5 min at an RF power of 50 W and a chamber pressure of 10 mTorr. The sheet resistances of the samples were then measured using a four-point probe. The resistances of the samples were measured again after an additional minute of etching, corresponding to a total etch time of 3.5 min. To get a better sense of how the measured sheet resistances reflected the etching process, the resistances were converted into inferred film thicknesses using the conversion  $d = \rho/R_s$ , where  $d$  is the remaining film thickness,  $R_s$  is the sheet resistance, and  $\rho$  is the resistivity. An estimate of  $\rho$  was obtained by using x-ray reflectometry to measure the thickness of a sister film with the same sheet resistance as the samples under investigation and calculating the resistivity using the expression above. From this approach, we obtained a value of  $\rho = 2.5 \text{ k}\Omega \text{ nm}$ , which is consistent with the results for an  $\sim 5$  nm film reported in prior work.<sup>12</sup> Given the agreement between values, we assumed a constant resistivity across all of the samples for the sake of simplicity, allowing us to compare inferred film thicknesses between samples.

### B. Results and discussion

Figure 3 shows the inferred remaining NbN film thickness as a function of exposure time to the TMAH after each of the etch trials. In comparison to the undeveloped control sample, those that had been exposed to TMAH for 30–90 s and rinsed with the standard 30 s DI water procedure had noticeably greater film thicknesses after the 2.5 min etch; this difference in film thickness indicates that the processed films were less etched than the control film, as we had initially observed in the patterned chip that first motivated this study. The difference in thickness between the control and exposed samples slightly increased after an additional minute of etching, implying that a type of barrier to etching was present on the treated films.

Interestingly, subjecting the treated samples to a 3 min DI water rinse under a running stream proved to significantly reduce the discrepancy in remaining film thickness of the treated films with respect to the control. Whereas treated samples that were rinsed for 30 s differed in thickness from the control by about 7–8 nm, those that underwent the vigorous rinse were within 2 nm of the untreated sample film thickness. This result suggests that the material that formed the barrier to etching was water soluble. However, it should be noted that simply submerging treated samples in DI water for 3–5 min had no noticeable improvement over the 30 s rinsing process, suggesting that a constant resupply of DI water on the film surface is necessary to remove the barrier. This is consistent with prior studies comparing immersion cleaning to direct spraying, which have found that a steady

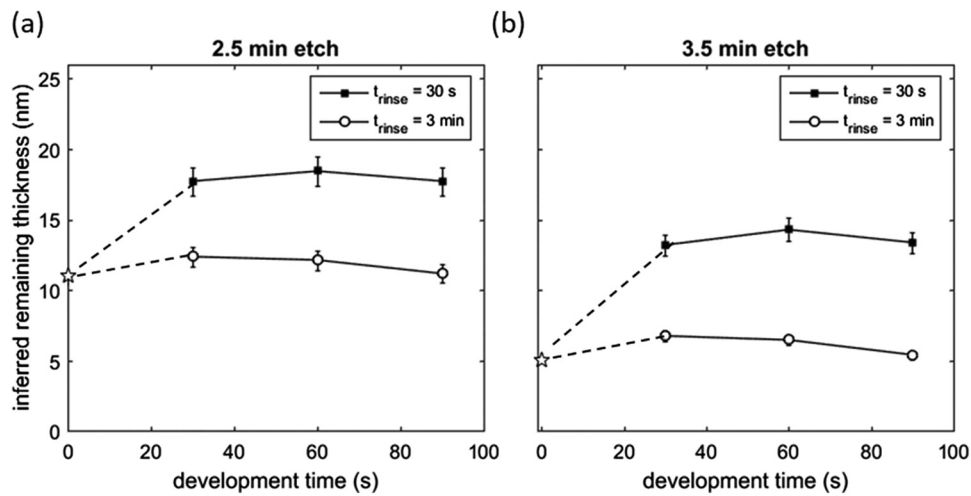


Fig. 3. Impact of TMAH development on the reactive ion etching rate of bare NbN films. Plots show the remaining film thickness vs exposure time to 25% TMAH. Thicknesses (inferred from sheet resistances) were measured after (a) 2.5 min and (b) 3.5 min of RIE. The solid squares indicate that the development was stopped by a 30 s DI rinse (the traditional procedure), while the open circles indicate that the samples were subjected to a vigorous 3 min DI rinse. The star connected by dashed lines represents the untreated control sample. Error bars represent  $\pm\frac{1}{2}\sigma$ , where  $\sigma$  is the standard deviation of the four-point resistance measurement.

water flow improves rinsing by continuously exposing the film surface to fresh solutions and allowing more efficient penetration into the material through shear force from the stream.<sup>13–15</sup>

Additionally, the remaining thicknesses of the samples that were vigorously rinsed for 3 min hint at the possibility of the NbN film being thinned by the development process. If the etch barrier was indeed removed by the DI rinsing, the lower remaining thickness of the sample developed for 90 s in comparison to those that were developed for 30 and 60 s implies that it had a thinner initial film thickness before the etching took place, assuming the etch rate was the same between the samples. As a result, it is apparent that exposure to TMAH not only creates a barrier to the etching of NbN films but also makes a physical change on the film itself.

### III. EXPERIMENT 2: MATERIAL ANALYSIS

#### A. Methods

In order to explain the observed reactive ion etching trends shown in Fig. 3, we analyzed the composition of the etch barrier and measured the superconducting properties of NbN films exposed to TMAH. Changes to the superconducting properties of the films were studied by measuring the  $R_s$  and  $T_c$  of samples as a function of exposure time to 25% TMAH. To maximize the observable change with respect to the initial film thickness, we sputtered a thinner film than used previously ( $d = 5 \text{ nm}$ ,  $R_s = 600 \Omega/\text{square}$ ); sheet resistances of this magnitude are similar to those of NbN films used for SNSPDs, making this study further relevant to the fabrication of standard superconducting devices. Samples of the film were then submerged in 25% TMAH for durations ranging from 1 min to 25 h, followed by a vigorous 3 min DI rinse to remove the etch barrier species. Afterwards, the sheet resistance and critical temperature of each of the samples were measured. As before,  $R_s$  measurements were

converted into inferred film thicknesses; for these films,  $\rho$  was estimated to be  $2.9 \text{ k}\Omega\cdot\text{nm}$  from x-ray reflectometry measurements of a sister film. A control sample with no TMAH exposure was also evaluated.

Analysis of the etch barrier composition was performed using Fourier transform infrared (FTIR) spectroscopy operated in the attenuated total reflection (ATR) mode. The sample was prepared by sputtering a thick NbN film of the same properties ( $R_s = 90 \Omega/\text{square}$ ) as those used in Fig. 3 on an Si wafer. The full wafer was submerged in 25% TMAH for 4 h. To collect a film of the etch barrier, the wafer was sonicated in DI water for 20 min and rinsed in IPA. A solution of the sonicated bath was left to evaporate for 3 days, resulting in a dense liquid with visible clusters of material. Drops of this solution were then pipetted onto a clean Si wafer and dried on a hotplate at  $90^\circ\text{C}$  for 5 min to remove excess solvents. A Thermo Fisher Continuum Fourier Transform Infrared Microscope was used to collect spectra of the dried material.

#### B. Results and discussion

Figures 4(a) and 4(b) display the changes in superconducting film parameters that occurred with increased exposure to 25% TMAH. Exposing the film for as little as 60 s—a common development time—led to a 0.25 nm or 5% decrease in film thickness, and 0.2 K decrease in  $T_c$ . In the extreme case of 25 h of exposure, the film thickness decreased by nearly 3 nm or nearly 57%, and the  $T_c$  decreased by roughly 1.6 K. These results suggest that the film is thinned by TMAH and that even short exposure times are sufficient to degrade the superconducting film. Additionally, the absence of saturation in the trends of Figs. 4(a) and 4(b) implies that the reaction between TMAH and the film does not only involve the thin ( $\sim 1\text{--}2 \text{ nm}$ ) layer of oxide that grows on the NbN surface, which would cause the



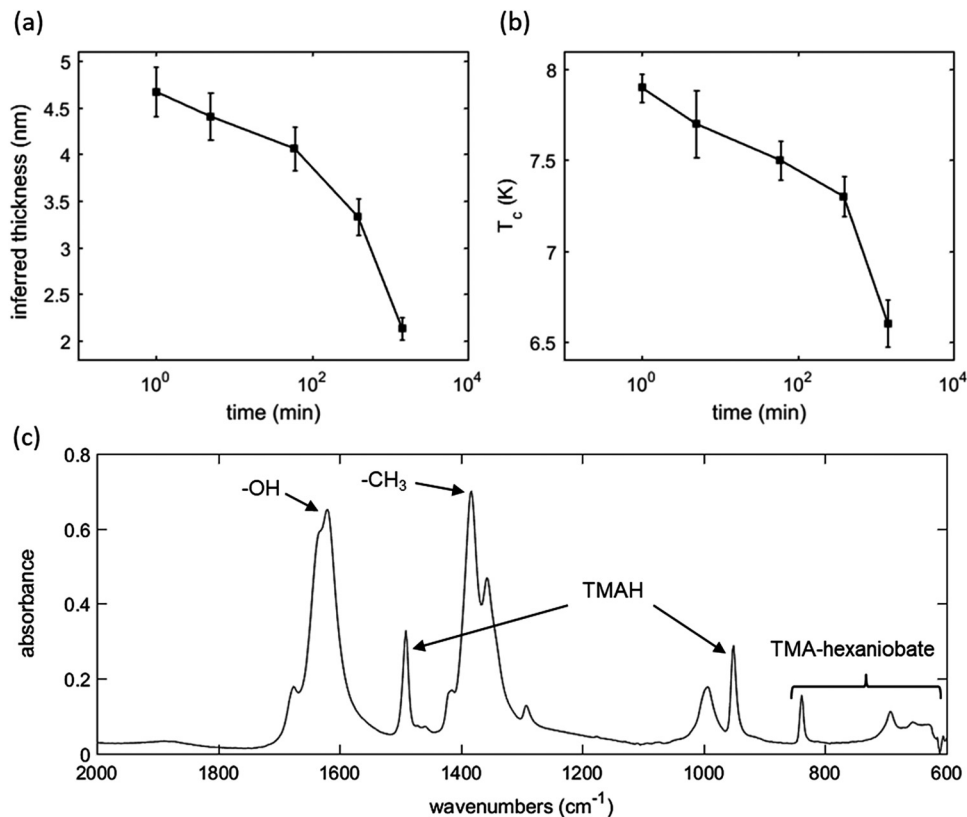


FIG. 4. Evidence of reaction involving NbN. (a) Inferred film thickness of a thin NbN film for various 25% TMAH development times, plotted on a log scale. The thickness continues to decrease for development times as long as 25 h. Error bars represent  $\pm 1/2\sigma$ , where  $\sigma$  is the standard deviation of the four-point resistance measurement. (b) Critical temperature for the same samples as shown in (a). Error bars represent  $\pm 1/2\sigma$ , where  $\sigma$  is the standard deviation of the critical temperature measurement. (c) ATR-FTIR spectrum of precipitate from a thick ( $\sim 20$  nm) NbN film left in 25% TMAH for 4 h. The spectrum reveals peaks corresponding to reported values for a TMA-hexaniobate salt.

trend to plateau soon after the oxide was consumed, but rather involves the entire superconducting film.

This change may be better understood through the ATR-FTIR spectrum of the precipitated etch barrier shown in Fig. 4(c). In addition to peaks characteristic of TMAH at 1490 and 951  $\text{cm}^{-1}$ , there are low lying peaks at 838, 692, and 650  $\text{cm}^{-1}$ . These peaks were found to be in agreement with three of the main signatures in the spectrum of a TMA-hexaniobate salt ( $[(\text{CH}_3)_4\text{N}]_5[\text{H}_3\text{Nb}_6\text{O}_{19}] \cdot 20\text{H}_2\text{O}$ ), which has recently been synthesized by reacting hydrous niobium oxide  $\text{Nb}_2\text{O}_5$  with TMAH in solution.<sup>16</sup> Remaining peaks around 1620 and 1383  $\text{cm}^{-1}$  may correspond to the typical signatures of surface hydroxyl groups from absorbed water<sup>17–20</sup> and C-H bending of methyl species,<sup>21,22</sup> respectively, while the peak at 1000  $\text{cm}^{-1}$  may represent the native oxide of the silicon substrate.<sup>23,24</sup>

Identification of TMA-hexaniobate as the primary etch barrier material explains several of the phenomena reported in this study. First, the intrinsic water solubility of the salt accounts for the ability to remove the etch barrier through a vigorous DI water rinse. Additionally, Ref. 16 showed that TMA-hexaniobate readily forms clusters with itself, which could manifest in the enhanced surface roughness of the treated film displayed in Fig. 2. Finally, an etch barrier formed from a reaction that involves Nb would account for the measured deterioration in thickness and  $T_c$  that indicated a reduction of the pure NbN film; it would also explain the similar deterioration caused by TMAH pretreatment that was reported in Ref. 10. Thus, information from the IR spectrum elucidates the mechanism behind our previous observations, which is conceptually presented in Fig. 5.

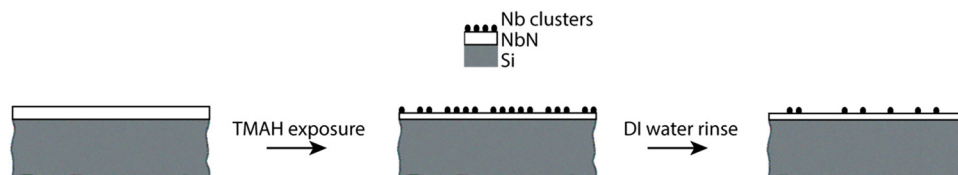


FIG. 5. Conceptual illustration of surface modification by TMAH. Exposing the NbN film to 25% TMAH leads to a reaction that produces TMA-hexaniobate clusters, thinning the pure NbN film and creating a barrier to reactive ion etching. However, a sufficiently vigorous DI water rinse removes the clusters, leaving an NbN film that is thinner than the initial state.

Although there remains some debate about the precise dynamics dictating the etching of NbN in CF<sub>4</sub>, there are certain means through which the presence of the TMA-hexaniobate salt could interfere with the etching process. Research on reactive ion etching with CF<sub>4</sub> has shown that polymerization occurs as the amount of available fluorine decreases, forming unsaturated polymers that more readily adhere to surfaces.<sup>25</sup> This effect can be enhanced by the presence of hydrogen, producing polymer deposits such as CHF<sub>x</sub> and blocking the underlying substrate from being etched.<sup>26</sup> Reduced etching via plasma polymerization has also been observed in molybdenum, which reacted with chemisorbed fluorocarbon radicals to form an etch-stop.<sup>27</sup> As Nb and Mo are both refractory metals, it is possible that a similar process is occurring in our samples. The TMA-hexaniobate salt may also be slowing the etch by consuming the reactant that dominates the chemical etching of NbN. Past work suggests that active atomic fluorine etches NbN by reacting to form volatile fluorides;<sup>28</sup> however, the etch rate was observed to decrease in the presence of CHF<sub>3</sub> and CH<sub>4</sub>, which reduced the amount of available active fluorine by participating with it in a reaction.<sup>29</sup> Thus, it is possible that the TMA-hexaniobate salt reacts with CF<sub>4</sub> to form a polymer barrier that blocks the physical etching of NbN while also limiting the chemical etch by consuming the principal reactant. While beyond the scope of this work, further surface analysis and study of the reactive ion etching process are needed to confirm these suspicions.

#### IV. CONCLUSIONS

In this work, we have seen that the 25% TMAH developer used in standard HSQ patterning adversely affects NbN films by reacting with the superconductor to form an Nb-based salt that creates a barrier to etching in CF<sub>4</sub>. We demonstrated that the etch barrier forms even for development times as short as 30 s, but that it can be removed through vigorous DI water rinsing. This approach offers a workable solution to the pattern transfer issues we encountered in thick NbN films; however, it does not prevent the initial film deterioration that takes place as a consequence of the reaction between TMAH and NbN. While an HSQ mask can protect the top face of a structure during development, the sides of the pattern would remain vulnerable, threatening the quality of a particularly thin or narrow feature. Our work also reveals that processes which use a 25% TMAH pretreatment before spinning HSQ in order to promote adhesion deteriorate the quality of the NbN films before patterning even takes place. For particularly thin films like those used in the fabrication of SNSPDs, even minor deterioration of the surface could bear significant consequences on device performance.

Given these limitations, it would be beneficial to evaluate if more dilute TMAH-based developers (e.g., MF CD-26) have the same effect or if they could be used as substitutes in standard processes that employ 25% TMAH. Alternative developers of HSQ such as salty developers<sup>30</sup> may be used, but their influence on superconducting films has not yet been reported. It may also be desirable to investigate if other etch

processes such as Ar ion milling or Cl<sub>2</sub> reactive ion etching could replace CF<sub>4</sub> in order to avoid the vigorous 3 min DI water rinse required to remove the etch barrier. Finally, adding a protective layer between the NbN and HSQ could be used to prevent direct contact with the developer.

While further work is needed to create an HSQ fabrication process that poses no harm to NbN films, this study nonetheless explores steps that can be taken to classify and ameliorate an unknown etch contaminant in superconducting materials. By using FTIR, it was possible to obtain a spectrum of the precipitated contaminant, while measurements of film parameters, etch characteristics, and surface features provided evidence to support the contaminant's identity. Although this investigation has been specific to NbN, it is possible that other materials such as tantalum undergo similar processes, motivating the need for future studies of the same nature on a wide range of films.

#### AUTHOR CONTRIBUTIONS

E.T. and M.C. performed the experiments, analyzed the data, and wrote the paper with input from K.B.N.A. who took the micrographs of Fig. 2. K.B. supervised the project.

#### ACKNOWLEDGMENTS

The authors thank Lauren Fullmer for her guidance and Di Zhu, Andrew Dane, Owen Medeiros, the entire Quantum Nanostructures and Nanofabrication group, and Andrew Wagner for scientific discussions. They would also like to thank Tim McClure of the MIT Center for Materials Science and Engineering and James Daley of the MIT Nanostructures Laboratory for technical support. Additionally, the authors thank the reviewers for providing suggestions that made significant improvements to the manuscript. This research is based on work supported by the Office of the Director of National Intelligence (ODNI) and Intelligence Advanced Research Projects Activity (IARPA), via Contract No. W911NF-14-C0089. The views and conclusions contained herein are those of the authors and should not be interpreted as necessarily representing the official policies or endorsements, either expressed or implied, of the ODNI, IARPA, or the U.S. Government. The U.S. Government is authorized to reproduce and distribute reprints for Governmental purposes notwithstanding any copyright annotation thereon. Emily Toomey was supported by the National Science Foundation Graduate Research Fellowship Program (NSF GRFP) under Grant No. 1122374. Navid Abedzadeh was supported by the Natural Sciences and Engineering Research Council of Canada (NSERC) under the Postgraduate Scholarship-Doctoral Grant (PGSD3).

<sup>1</sup>G. N. Gol'tsman *et al.*, *Appl. Phys. Lett.* **79**, 705 (2001).

<sup>2</sup>H. L. Hortensius, E. F. C. Driessen, T. M. Klapwijk, K. K. Berggren, and J. R. Clem, *Appl. Phys. Lett.* **100**, 182602 (2012).

<sup>3</sup>A. N. McCaughan, N. S. Abebe, Q.-Y. Zhao, and K. K. Berggren, *Nano Lett.* **16**, 7626 (2016).

<sup>4</sup>A. E. Grigorescu and C. W. Hagen, *Nanotechnology* **20**, 292001 (2009).

<sup>5</sup>J. K. W. Yang *et al.*, *IEEE Trans. Appl. Supercond.* **15**, 626 (2005).

- <sup>6</sup>W. Henschel, Y. M. Georgiev, and H. Kurz, *J. Vac. Sci. Technol. B* **21**, 2018 (2003).
- <sup>7</sup>J. K. W. Yang *et al.*, *J. Vac. Sci. Technol. B* **27**, 2622 (2009).
- <sup>8</sup>X.-L. Han, G. Larrieu, and E. Dubois, *J. Nanosci. Nanotechnol.* **10**, 7423 (2010).
- <sup>9</sup>K. Mohammad Moniruzzaman, Development of a single-step fabrication process for nanoimprint stamps (2011).
- <sup>10</sup>F. Najafi *et al.*, *IEEE J. Sel. Top. Quantum Electron.* **21**, 1 (2015).
- <sup>11</sup>D. Fan and Y. Ekinci, *Proc. SPIE* **9776**, 97761V (2016).
- <sup>12</sup>A. E. Dane *et al.*, *Appl. Phys. Lett.* **111**, 122601 (2017).
- <sup>13</sup>W. Kern, *J. Electrochem. Soc.* **137**, 1887 (1990).
- <sup>14</sup>J. Bardina, *Part. Sci. Technol.* **6**, 121 (1988).
- <sup>15</sup>A. A. BUSnaina and F. Dai, *J. Adhes.* **67**, 181 (1998).
- <sup>16</sup>L. B. Fullmer, R. H. Mansergh, L. N. Zakharov, D. A. Keszler, and M. Nyman, *Cryst. Growth Des.* **15**, 3885 (2015).
- <sup>17</sup>M. Van Thiel, E. D. Becker, and G. C. Pimentel, *J. Chem. Phys.* **27**, 486 (1957).
- <sup>18</sup>A. Litke, Y. Su, I. Tranca, T. Weber, E. J. M. Hensen, and J. P. Hofmann, *J. Phys. Chem. C* **121**, 7514 (2017).
- <sup>19</sup>T. Fuchigami and K. Kakimoto, *J. Mater. Res.* **32**, 3326 (2017).
- <sup>20</sup>F. de O. Cantão, W. de C. Melo, L. C. A. Oliveira, A. R. Passos, and A. C. da Silva, *Quím. Nova* **33**, 528 (2010).
- <sup>21</sup>L. Andrews and G. C. Pimentel, *J. Chem. Phys.* **47**, 3637 (1967).
- <sup>22</sup>B. Nolin and R. N. Jones, *Can. J. Chem.* **34**, 1382 (1956).
- <sup>23</sup>R. T. Conley, *Infrared Spectroscopy*, 1st ed. (Allyn and Bacon, Inc., Boston, MA, 1966), pp. 176–178.
- <sup>24</sup>P. Gupta, A. C. Dillon, A. S. Bracker, and S. M. George, *Surf. Sci.* **245**, 360 (1991).
- <sup>25</sup>W. W. Stoffels, E. Stoffels, and K. Tachibana, *J. Vac. Sci. Technol. A* **16**, 87 (1998).
- <sup>26</sup>J. H. Thomas, X. C. Mu, and S. J. Fonash, *J. Electrochem. Soc.* **134**, 4 (1987).
- <sup>27</sup>S.-J. Park, C. P. Sun, J. T. Yeh, J. K. Cataldo, and N. Metropoulos, *MRS Proc.* **68**, 65 (1986).
- <sup>28</sup>A. C. Seabra, P. Verdonck, W. L. Xavier, and V. Baranauskas, *Proc. SPIE* **1185**, 80 (1990).
- <sup>29</sup>X. F. Meng, R. S. Amos, A. W. Lichtenberger, R. J. Mattauch, and M. J. Feldman, *IEEE Trans. Magn.* **25**, 1239 (1989).
- <sup>30</sup>J. K. W. Yang and K. K. Berggren, *J. Vac. Sci. Technol. B* **25**, 2025 (2007).